CERN-PH-TH/2004-123
ROMA - 1399/04
SHEP 04-21

Manifestly gauge invariant QED

Stefano Arnone,[¶] Tim R. Morris [†] and Oliver J. Rosten[†]

[¶]Dipartimento di Fisica, Università degli Studi di Roma "La Sapienza"
P.le Aldo Moro, 2 - 00185 Roma, Italy

[†]School of Physics and Astronomy, University of Southampton,
Highfield, Southampton SO17 1BJ, U.K.

E-mails: Stefano.Arnone@roma1.infn.it,
T.R.Morris@soton.ac.uk, O.J.Rosten@soton.ac.uk

Abstract

We uncover a method of calculation that proceeds at every step without fixing the gauge or specifying details of the regularisation scheme. Results are obtained by iterated use of integration by parts and gauge invariance identities. Calculations can be performed almost entirely diagrammatically. The method is formulated within the framework of an exact renormalisation group for QED. We demonstrate the technique with a calculation of the one-loop beta function, achieving a manifestly universal result, and without gauge fixing.

Contents

1 Introduction and Conclusions

The purpose of this paper is to illustrate a novel methodology which has been developed for Yang-Mills theory, in the simpler context of (massless) QED. In [1], a manifestly gauge invariant Exact Renormalisation Group (ERG) was introduced, suitable for computation in $SU(N)$ gauge theory, to one-loop, without the need for gauge fixing. The formalism has now been refined to facilitate computation to arbitrary loop order [2, 3]. Indeed, the (universal) $SU(N)$ Yang-Mills two-loop β-function has been successfully calculated [3], representing the very first continuum two-loop calculation to be done in Yang-Mills theory, without fixing the gauge. This paper provides an introduction to these ideas, whilst bypassing many of the technical subtleties. We will see that it is thus straightforward to adapt these manifestly gauge invariant methods to the case of perturbative computations in QED.

To treat QED within the framework of the manifestly gauge invariant ERG, we must adopt a regularisation scheme which incorporates a gauge invariant, real cutoff, Λ. Whereas this is a source of much of the complication in the non-Abelian case [4],

it is straightforward for QED. The pure gauge part of the theory can be regulated by supplementing the kinetic term with a cutoff function, c, which dies off sufficiently fast at high energies. To regulate the fermionic part of the action, we introduce an unphysical, commuting spinor field, χ, with a mass at the cutoff scale, which provides Pauli-Villars regularisation.

When providing regularisation by Pauli-Villars fields, one has to provide a prescription for adding together the separately ultraviolet divergent pieces. Here this is easily solved by the traditional method of momentum routing, i.e. we ensure that the loop momentum assignments for every χ loop are the same as the assignments in the corresponding physical fermion loop [4]. In fact, as we will see, such a routing is embedded in the techniques described in this paper since the corresponding diagrams are represented as one diagram, with internal fields summed over.

However, to reflect the more involved case of a flow equation for $SU(N)$ Yang-Mills theory where the $SU(N|N)$ regularisation requires a preregularisation, we use dimensional regularisation as a preregularisation.[1] Working in general dimension, D, will prove particularly convenient as this allows an efficient means of extracting the numerical value of β-function coefficients (see section 5.3.2). The regularisation scheme is fully described in appendix A.

Having cast QED in a form suitable for the ERG in section 2, in section 3.1 we formulate the flow equation, which describes how the effective action, $S \equiv S_\Lambda$, changes with Λ. Using the insights of [5] into general ERGs and our experiences in both the non-Abelian case [1] and scalar case [6], an appropriate equation can simply be written down. Indeed, there are an infinite number of flow equations we can use, from each of which we can extract equivalent physics. The key point is that all of these equations must satisfy the following properties.

First, the flow equation must be gauge invariant. That we are able to formulate gauge invariant ERGs turns out to have a wonderful benefit: calculations can be performed without gauge fixing [1, 3, 7]. In QED (and non-Abelian gauge theory), the exact preservation of gauge invariance means that the connection does not renormalise. By scaling the coupling out of the connection, the gauge field does not renormalise (though we note that the fermion and unphysical regulator fields do suffer wavefunction renormalisation).

Secondly, all ingredients of the flow equation must be infinitely differentiable in momenta. This property, referred to as quasilocality [8], guarantees that each RG step $\Lambda \mapsto \Lambda - \delta\Lambda$ does not generate IR singularities [9]; equivalently that Kadanoff blocking takes places only over a localised patch.

[1] There are encouraging indications [3] that an entirely diagrammatic prescription can instead be adopted for $SU(N)$ Yang-Mills theory, which would make sense not only in general D but also in D strictly equal to four.

Thirdly, the flow is self-similar [10], which demands that the effective action depend only on the scale Λ, through its couplings (this can be straightforwardly extended to massive theories [8]). By definition, such actions lie on a Renormalised Trajectory guaranteeing, amongst other things, the existence of a continuum limit [11].

Lastly, the partition function must be left invariant under the flow: e^{-S} should transform into a total derivative. This ensures that, starting with some quantum field theory at a high scale, our effective action is guaranteed to still be describing the same physics at a very much lower scale (implicitly assuming the second point, above).

In turn, these features imply that our flow equation possesses other properties. Indeed, it follows that our flow equation does correspond to integrating out [2, 7]. Furthermore, locality and that we are really dealing with QED at all scales—two properties which are generally not manifest in the Wilsonian effective action at some finite value of Λ—are guaranteed (at least in perturbation theory) [1].

When we explicitly construct the flow equation (see equations (12)–(14)), we will see that it depends not just on the Wilsonian effective action but also on a second functional $\hat{S}$, the 'seed action' [1, 6]. This object controls the flow and represents the continuum version of the choice of blocking transformations in the application of Wilsonian RG techniques to latticised problems [9, 12]. Like the Wilsonian effective action, the seed action must be gauge invariant and infinitely differentiable. However, whereas we solve the flow equations for the former, the latter acts as an input.

Now, so long as our choice of $\hat{S}$ is consistent with our approach, we are free to choose it to be whatever we like. However, we expect the result of a computation of some universal quantity to be independent of this choice and, indeed, our choice of cutoff function, c.

That a calculation must yield a result independent of the precise details of particular ingredients leads to a highly constrained calculational procedure. Generally speaking, the only way to remove dependence on an instance of an unspecified component of $\hat{S}$ is for there to be a second instance, of opposite sign. Indeed, this is so constraining that calculations can be performed almost entirely diagrammatically.

Whilst the freedom to leave the seed action largely unspecified has guided us to an efficient calculational procedure we have, in some sense, complicated the issue by not using the simplest seed action suitable for our purposes. The most obvious resolution to this is to simply regard the freedom of the seed action as scaffolding: it has guided us to an efficient calculational procedure, but now we can dispense with it, keeping the procedure but choosing the simplest form for the seed action, consistent with our approach.

However, there is a more sophisticated way of looking at things. Certainly, for the calculation of β-function coefficients—*to any order in perturbation theory*—it is possible to show that explicit dependence on $\hat{S}$ is guaranteed to cancel out [3, 13].

Thus, at least up until this stage of a calculation, where any remaining seed action dependence is now implicit, it makes no difference how complicated a seed action has been chosen; we can simply bypass the entire procedure of cancelling explicit instances of seed action components.

A second benefit of a general seed action is that, by making certain judicious choices, we can simplify the calculation procedure employed within the ERG. Specifically, we choose to set the classical, two-point Wilsonian effective action vertices equal to the corresponding seed action vertices. A direct consequence of this is that the classical two-point vertices are now related, in a particularly simple way, to the integrated ERG kernel. This leads to the so-called 'effective propagator relationship', which is central to our entire diagrammatic approach.

The diagrammatics are introduced in section 3.2 and then specialised to the weak coupling regime in sections 4 and 4.2. This prepares us for the final section, 5, in which we illustrate how to use the formalism to perform actual calculations, by computing the QED one-loop β-function, without fixing the gauge or specifying the non-universal details of either $\hat{S}$ or c.

2 Adapting QED for the ERG

We denote the gauge field by A_μ, the physical fermion field by ψ and the unphysical regulating field by χ. The covariant derivative is

$$\nabla_\mu = \partial_\mu - iA_\mu, \tag{1}$$

where it is apparent that we have scaled the renormalised coupling, e, out of this definition. The renormalised coupling, e, and the canonical normalisation of the spinor fields are defined through the renormalisation condition

$$S = \frac{1}{e^2}\int d^D x \, \left(\frac{1}{4}F_{\mu\nu}^2 + \bar{\psi} i\partial\!\!\!/ \psi + \bar{\chi} i\partial\!\!\!/ \chi + \cdots,\right) \tag{2}$$

where $F_{\mu\nu} = i\left[\nabla_\mu, \nabla_\nu\right] = \partial_\mu A_\nu - \partial_\nu A_\mu$ is the field strength and the ellipsis denotes higher dimension operators (and the ignored vacuum energy). The mass of the physical fermion is set to zero implicitly by ensuring that there is no other physical scale apart from Λ, which itself tends to zero as all momentum modes are integrated out.

The effective action can be written

$$S = \sum_{n=2}^{\infty} \frac{1}{s_n} \int d^D x_1 \cdots d^D x_n \, S^{X_1 \cdots X_n}_{a_1 \cdots a_n}(x_1, \ldots, x_n) X_1^{a_1}(x_1) \cdots X_n^{a_n}(x_n), \tag{3}$$

where X represents any of A_μ, ψ or χ; the indices a_i being Lorentz indices or spinor indices, as appropriate. Each vertex must possess a minimum of two fields and those vertices possessing instances of $\psi(\chi)$ without a matching $\bar{\psi}(\bar{\chi})$ are given a value of zero. For each list, $X_1 \cdots X_n$, only one permutation of the fields appears in the sum; moreover, we will take the anticommuting ψ, $\bar{\psi}$s to be *canonically ordered*, by which we mean they always occur in the order $\bar{\psi}\bar{\psi}\cdots\psi\psi$. The symmetry factor of each vertex is $s_n = \prod_f n_f!$, where n_f is the number of fields of type f and $f = A,\ \psi,\ \bar{\psi},\ \chi,\ \bar{\chi}$.

We write the momentum space vertices as

$$S^{X_1\cdots X_n}_{a_1\,\ldots\,a_n}(p_1,\ldots,p_n)\,(2\pi)^D\,\delta\left(\sum_{i=1}^{n} p_i\right)$$
$$= \int d^D x_1 \cdots d^D x_n\, e^{-i\sum_i x_i\cdot p_i}\, S^{X_1\cdots X_n}_{a_1\,\ldots\,a_n}(x_1,\ldots,x_n),$$

where all momenta are taken to point into the vertex. We will employ the shorthand

$$S^{X_1X_2}_{a_1\,a_2}(p) \equiv S^{X_1X_2}_{a_1\,a_2}(p,-p). \tag{4}$$

The effective action (3) is invariant under the gauge transformation

$$\begin{aligned}
\delta\psi &= i\alpha(x)\psi, && (5)\\
\delta\bar{\psi} &= -i\bar{\psi}\alpha(x), && (6)\\
\delta\chi &= i\alpha(x)\chi, && (7)\\
\delta\bar{\chi} &= -i\bar{\chi}\alpha(x), && (8)\\
\delta A_\mu &= \partial_\mu\alpha(x). && (9)
\end{aligned}$$

Notice that by scaling the coupling constant out of (1), we ensure that A_μ does not suffer from any wavefunction renormalisation. If A_μ were to acquire a wavefunction renormalisation then, on replacing A_μ by $Z^{1/2}A_\mu$, it is clear that, in order not to violate (9), we must re-parametrise α as well. However, re-parameterising α is inconsistent with (5)–(8) even taking into account the wavefunction renormalisation for the physical fermion and unphysical regulator field.

Invariance of the effective action, (3), under the transformations (5)–(9) implies the following Ward identities. First, pure-A vertices are transverse on all legs:

$$p_i^{\mu_i}\, S^{A\,\cdots A\,\cdots A}_{\mu_1\cdots\mu_i\cdots\mu_m}(p_1,\ldots,p_i,\ldots,p_m) = 0, \qquad \forall p_i^{\mu_i}. \tag{10}$$

Secondly, vertices containing ψs and / or χs and at least one gauge field are related to vertices with one less gauge field. It is useful to define the field Φ to be

either ψ or χ; in the former (latter) case, $\bar{\Phi}$ should be identified with $\bar{\psi}$ ($\bar{\chi}$). The Ward identity is:

$$k^\mu S^{AA\cdots A\ \bar{\Phi}_1\cdots\bar{\Phi}_m\Phi_1\cdots\Phi_m}_{\mu\,\mu_1\cdots\mu_n a_1\cdots a_m\ b_1\cdots b_m}(k,p_1,\ldots,p_n,q_1,\ldots,q_m,r_1,\ldots,r_m) =$$

$$\sum_i\Big\{S^{A\cdots A\ \bar{\Phi}_1\cdots\bar{\Phi}_m\Phi_1\cdots\Phi_i\cdots\Phi_m}_{\mu_1\cdots\mu_n a_1\cdots a_m\ b_1\cdots b_i\cdots b_m}(k,p_1,\ldots,p_n,q_1,\ldots q_m,r_1,\ldots,r_i+k,\ldots,r_m)$$

$$-S^{A\cdots A\ \bar{\Phi}_1\cdots\bar{\Phi}_i\cdots\bar{\Phi}_m\Phi_1\cdots\Phi_m}_{\mu_1\cdots\mu_n a_1\cdots a_i\cdots a_m\ b_1\cdots b_m}(k,p_1,\ldots,p_n,q_1,\ldots,q_i+k,\ldots q_m,r_1\ldots r_m)\Big\}. \quad (11)$$

The above generalises the well-known relation, $p^\mu S^{A\bar{\psi}\psi}_\mu(p,q,r) = S^{\bar{\psi}\psi}(q) - S^{\bar{\psi}\psi}(r)$, where the shorthand (4) has been used.

In addition to being invariant under gauge transformations, the action is charge conjugation invariant. In particular, this implies that any pure-A vertices carrying an odd number of fields vanish.

The seed action, $\hat{S}$, has a field expansion as in (3) and obeys the same symmetries as the Wilsonian effective action.

3 An ERG for QED

3.1 The Flow Equation

Our strategy is to write down a manifestly gauge invariant flow equation that incorporates the regularisation scheme outlined above. Following our previous works [1–3, 6, 7, 12, 14], we simply set (suppressing spinor indices)

$$\dot{S} + \gamma^{(\psi)}\left(\psi\frac{\delta S}{\delta\psi} + \bar{\psi}\frac{\delta S}{\delta\bar{\psi}}\right) + \gamma^{(\chi)}\left(\chi\frac{\delta S}{\delta\chi} + \bar{\chi}\frac{\delta S}{\delta\bar{\chi}}\right) = a_0[S,\Sigma_e] - a_1[\Sigma_e], \quad (12)$$

where $\dot{S} \equiv -\Lambda\partial_\Lambda S$ (in general dots above quantities will signify $-\Lambda\partial_\Lambda$), the γs take into account the contribution of the anomalous dimension of the spinor fields and $\Sigma_e \equiv e^2 S - 2\hat{S}$. The functionals $a_{0,1}$ are given by:

$$\begin{aligned} a_0[S,\Sigma_e] &= \frac{1}{2}\frac{\delta S}{\delta A_\mu}\cdot\dot{\Delta}^{AA}\cdot\frac{\delta\Sigma_e}{\delta A_\mu} + \frac{1}{2}\left(\frac{\delta\Sigma_e}{\delta\chi}\{\dot{\Delta}^{\bar{\chi}\chi}\}\frac{\delta S}{\delta\bar{\chi}} + \frac{\delta S}{\delta\chi}\{\dot{\Delta}^{\bar{\chi}\chi}\}\frac{\delta\Sigma_e}{\delta\bar{\chi}}\right) \\ &\quad -\frac{1}{2}\left(\frac{\delta\Sigma_e}{\delta\psi}\{\dot{\Delta}^{\bar{\psi}\psi}\}\frac{\delta S}{\delta\bar{\psi}} + \frac{\delta S}{\delta\psi}\{\dot{\Delta}^{\bar{\psi}\psi}\}\frac{\delta\Sigma_e}{\delta\bar{\psi}}\right) \quad (13) \\ a_1[\Sigma_e] &= \frac{1}{2}\frac{\delta}{\delta A_\mu}\cdot\dot{\Delta}^{AA}\cdot\frac{\delta\Sigma_e}{\delta A_\mu} + \frac{\delta}{\delta\chi}\{\dot{\Delta}^{\bar{\chi}\chi}\}\frac{\delta\Sigma_e}{\delta\bar{\chi}} - \frac{\delta}{\delta\psi}\{\dot{\Delta}^{\bar{\psi}\psi}\}\frac{\delta\Sigma_e}{\delta\bar{\psi}}. \quad (14) \end{aligned}$$

To define these expressions properly, we must define our notation. Let us start by looking at terms involving functional derivatives with respect to A. Under the gauge transformations (5)–(9), both $\delta S/\delta A_\mu$ and $\delta\Sigma_e/\delta A_\mu$ are invariant. Thus, construction of a gauge invariant term in the flow equation involving these objects is trivial. We write the A-sector term in compact form by utilising the following shorthand: for any two functions $f(x)$ and $g(y)$ and a momentum space kernel $W(p^2/\Lambda^2)$,

$$f\cdot W\cdot g=\iint d^Dx\,d^Dy\,f(x)\,W_{xy}\,g(y), \tag{15}$$

with W_{xy} being $\int\frac{d^Dp}{(2\pi)^D}\,W(p^2/\Lambda^2)e^{ip\cdot(x-y)}$.

In the ψ and χ-sectors, however, things are more complicated since $\delta S/\delta\chi$ and so on are not invariant under gauge transformations. To construct gauge invariant terms for the flow equation, we must covariantise (15). Thus, for the spinors $u_a(x)$ and $v_b(y)$ and kernel W_{ab}, the gauge invariant generalisation of (15) is [7]

$$\begin{aligned}u\{W\}v=\sum_{n=0}^{\infty}\int&d^Dx\,d^Dy\,d^Dx_1\cdots d^Dx_n\\&u_a(x)W_{ab\,\mu_1\cdots\mu_n}(x_1,\ldots,x_n;x,y)A_{\mu_1}(x_1)\cdots A_{\mu_n}(x_n)v_b(y),\end{aligned} \tag{16}$$

where the n-point vertex $W_{ab\,\mu_1\cdots\mu_n}(x_1,\ldots,x_n;x,y)$ is a vertex of the covariantised kernel, $\{W\}$. If $n=0$, we recover the original kernel: $W_{ab}(;x,y)\equiv W_{ab}(x,y)$.

In the flow equation, where u and v both involve a functional derivative, we use the field with respect to which this derivative is taken to label the kernels. The vertices of the ERG covariantised kernels $\{\dot\Delta^{XY}\}$ obey Ward identities similar to (11), though we will not require them in this paper.

The final point to make about the flow equation is that we can choose the kernel $\dot\Delta^{\bar\psi\psi}$ to be zero, which clearly simplifies the flow equation. Nonetheless, even given this choice, it is useful to retain these terms and to process them using the flow equation. As we will see when we describe the diagrammatics, this does not actually lead to any extra work since all sectors can be treated in parallel. Moreover, allowing the ψ-sector to shadow the χ-sector will enable us to extract actual numerical answers from the flow equation in a convenient manner by making the UV regularisation of the results manifest.

3.2 Diagrammatics

In this section, we will give a diagrammatic form for the flow equation. First, though, we must introduce the diagrammatics for the actions and the kernels. Referring back to (3), consider the vertex with n gauge fields. We represent the *vertex coefficient*

function—i.e. we do not include either the actual fields or the symmetry factor—as shown in figure 1. We henceforth refer to all lines emanating from a vertex as decorations.

$$S^{A\cdots A}_{\mu_1\cdots\mu_n}(p_1,\ldots,p_n) =$$

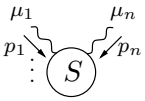

Figure 1: Example of the diagrammatic representation of a vertex coefficient function.

The argument of the vertex can be any action functional and so the vertices of $\hat{S}$ (or, indeed, Σ_e) have a similar diagrammatic interpretation. Inclusion of χs is straightforward. However, the order in which anticommuting fermionic decorations are read off is important: we always read off such that the algebraic form of the vertex is canonically ordered. Since we will never need to deal with external ψs or χs in this paper, we need not introduce a specific diagrammatic realisation. Rather, we will use solid lines to indicate dummy fields; these will appear as internal lines in diagrams, whence the possible fields they represent are summed over.

The diagrammatics for the vertices of the kernels is shown in figure 2; this time, we have not explicitly indicated the momentum flow but, once again, all momenta are taken to flow into the diagram. From (16) we note that only As decorate the kernel.

$$\dot{\Delta}^{X\,Y}_{a_1 a_2\,\mu_1\cdots\mu_n}(p_1,\ldots,p_n;r,s) =$$

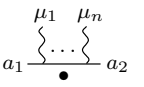

Figure 2: Diagrammatics for the vertices of the kernels

We now refine the diagrammatics. Consider the vertex coefficient function corresponding to the vertex decorated by some set of fields $\{f\}$. Rather than explicitly performing these decorations, it is useful to leave them implicit, as shown in figure 3.

Figure 3: A Wilsonian effective action vertex implicitly decorated by the set of fields $\{f\}$.

Using the notation of figure 3, the flow equation can now be cast in a particularly simple diagrammatic form, shown in figure 4. The terms on the r.h.s. are formed by a_0 and a_1, respectively.

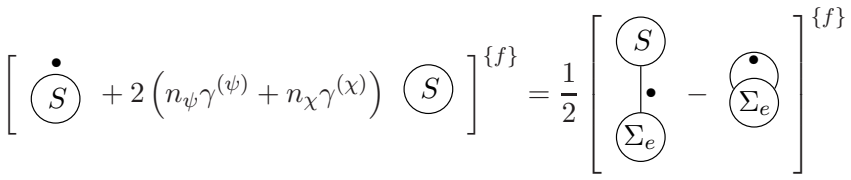

Figure 4: A diagrammatic representation of the flow equation.

The internal lines correspond to vertices of the kernels, where we sum over the fields at both ends. Decorating the diagrams of figure 4 is straightforward: we distribute the decorative fields $\{f\}$ in all independent ways over all structures. Note that, for particular choices of $\{f\}$, certain explicitly decorated structures will not exist; equivalently, we take the Feynman rule for such structures to be zero. For example, we know that the vertices of the kernel cannot be decorated by spinor fields.

Finally, we note that there are some additional rules for the term formed by a_1. If the internal line is in the χ-sector, we pick up a factor of two whereas, if it is in the ψ-sector, we pick up a factor of minus two.

By applying the flow equation iteratively (as we will do shortly) we can generate a diagram formed by the action of an arbitrary number of a_1s and a_0s. The Feynman rule for working out the sign of such arbitrarily complicated diagrams associated with internal ψs is simple and as expected: we pick up a sign for every loop. Note that loops can only ever be formed by a_1.

As an example, we compute the flow of a vertex decorated by two As (we will explicitly perform the decorations, rather than leaving them implicit), as shown in figure 5.

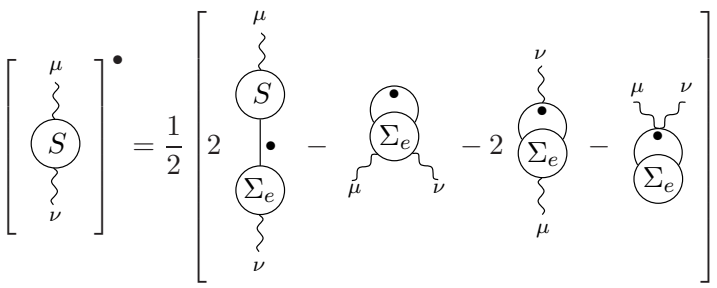

Figure 5: Example of using the diagrammatic flow equation.

Let us start by looking at the first term on the r.h.s. The internal line whose flavour, we recall, is summed over, must be in the A-sector. This diagram, like the third diagram on the r.h.s., comes with a relative factor of two, arising from combining the diagrams drawn as shown with those for which the A^1_μ and A^1_ν are swapped around (the two cases must be the same, by Bose symmetry). Note that no other diagrams can be formed by a_0, since these would necessarily possess a one-point vertex, which does not exist.

Let us now focus on the second term. The kernel can be in any sector. If we suppose that it is in the ψ-sector, then our previous rules determine the vertex to be $\Sigma_e^{\bar{\psi}\psi AA}$ and demand that we pick up a factor of -2. The third and fourth terms only exist when the internal line is in the χ or ψ-sectors.

We now introduce an additional piece of notation which allows us to perform an intermediate step between going from unrealised decorations parameterised by $\{f\}$ to explicitly decorated diagrams.

Suppose that we have a diagram for which we want to focus on the components possessing a two-point vertex. So long as there is still at least one field sitting as an implicit decoration, we must specify that our vertex has precisely two decorations. We use a superscript on the vertex argument to denote this. Two examples are shown in figure 6.

In the first diagram, we see that we must use one and only one element of the set $\{f\}$ to decorate the bottom vertex. In the second diagram, the elements of $\{f'\}$ must be spread around the kernel and the top vertex.

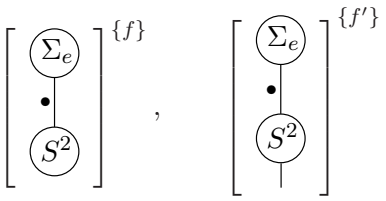

Figure 6: Forcing a vertex on an implicitly decorated diagram to have precisely two decorations.

4 The Weak Coupling Expansion

4.1 The Weak Coupling Flow Equation

In this section, we examine the form the flow equations take in the perturbative limit. Following [1, 7], the action has the weak coupling expansion

$$S = \sum_{i=0}^{\infty} \left(e^2\right)^{i-1} S_i = \frac{1}{e^2} S_0 + S_1 + \cdots, \tag{17}$$

where S_0 is the classical effective action and the $S_{i>0}$ the ith-loop corrections. The seed action has a similar expansion:

$$\hat{S} = \sum_{i=0}^{\infty} e^{2i} \hat{S}_i. \tag{18}$$

Note that these definitions are consistent with $\Sigma_e = e^2 S - 2\hat{S}$; identifying powers of e in the flow equation, it is clear that S_i and $\hat{S}_i$ will always appear together. With this in mind, we now define

$$\Sigma_i = S_i - 2\hat{S}_i. \tag{19}$$

The β-function takes the usual form:

$$\beta \equiv -\Lambda \partial_\Lambda e = \sum_{i=1}^{\infty} e^{2i+1} \beta_i. \tag{20}$$

and $\gamma^{(\psi)}$, $\gamma^{(\chi)}$ have the expansions

$$\gamma^{(\psi)} = \sum_{i=1}^{\infty} e^{2i} \gamma_i^{(\psi)}, \qquad \gamma^{(\chi)} = \sum_{i=1}^{\infty} e^{2i} \gamma_i^{(\chi)}. \tag{21}$$

We now substitute expansions (17), (18), (20) and (21) into equation (12) and, using equation (19), obtain the weak coupling expansion of the flow equation:

$$\dot{S}_n = \sum_{r=1}^{n} \left[2(n-r-1)\beta_r - \gamma_r^{(\psi)} \left(\psi \frac{\delta}{\delta\psi} + \bar{\psi} \frac{\delta}{\delta\bar{\psi}} \right) - \gamma_r^{(\chi)} \left(\chi \frac{\delta}{\delta\chi} + \bar{\chi} \frac{\delta}{\delta\bar{\chi}} \right) \right] S_{n-r} + \sum_{r=0}^{n} a_0 \left[S_{n-r}, \Sigma_r \right] - a_1 \left[\Sigma_{n-1} \right]. \tag{22}$$

We note that the classical term can be brought into a more symmetrical form. This follows from the invariance of $a_0[S_{n-r}, \Sigma_r] + a_0[S_r, \Sigma_{n-r}]$ under $r \to n-r$. We exploit this by recasting the classical term as follows:

$$\begin{aligned} a_0[\bar{S}_{n-r}, \bar{S}_r] &\equiv a_0[S_{n-r}, S_r] - a_0[S_{n-r}, \hat{S}_r] - a_0[\hat{S}_{n-r}, S_r]. \\ &= \begin{cases} \frac{1}{2} \left(a_0[S_{n-r}, \Sigma_r] + a_0[S_r, \Sigma_{n-r}] \right) & n-r \neq r \\ a_0[S_r, \Sigma_r] & n-r = r. \end{cases} \end{aligned} \tag{23}$$

Hence, we can rewrite the flow equation in the following form:

$$\dot{S}_n = \sum_{r=1}^{n} \left[2(n-r-1)\beta_r - \gamma_r^{(\psi)} \left(\psi \frac{\delta}{\delta\psi} + \bar{\psi} \frac{\delta}{\delta\bar{\psi}} \right) - \gamma_r^{(\chi)} \left(\chi \frac{\delta}{\delta\chi} + \bar{\chi} \frac{\delta}{\delta\bar{\chi}} \right) \right] S_{n-r} + \sum_{r=0}^{n} a_0 \left[\bar{S}_{n-r}, \bar{S}_r \right] - a_1 \left[\Sigma_{n-1} \right]. \tag{24}$$

When expressing this equation diagrammatically, we will abbreviate the argument of Wilsonian effective action vertices to just the loop order i.e. we replace S_m by just m. Similarly, we represent seed action vertices by, e.g., $\hat{m}$.

4.2 The Effective Propagator Relation

Central to our diagrammatic approach is the relationship between the two-point, tree level vertices and the integrated ERG kernels—the 'effective propagator relation'. To investigate this, we use the flow equations. First, we specialise equation (22) or (24) to $n = 0$:

$$\dot{S}_0 = a_0[S_0, \Sigma_0]. \tag{25}$$

Next we further specialise to consider the flow of all two-point vertices, as shown in figure 7.

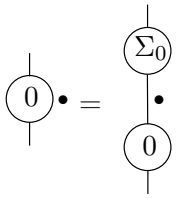

(26)

Figure 7: Flow of all possible two-point, tree level vertices.

We can now solve equation (26), giving an expression for the Wilsonian effective action, two-point, tree level vertices in terms of the seed action two-point, tree level vertices and the zero-point kernels.

Our strategy is to follow [1, 6] and utilise the freedom inherent in $\hat{S}$ by choosing the two-point, tree level components of $\hat{S}$ to be equal to the corresponding components of S i.e.

$$\hat{S}_{0RS}^{\ f\,f}(k) = S_{0RS}^{\ f\,f}(k), \tag{27}$$

where the indices R and S are either Lorentz indices or spinor indices, as appropriate. We emphasise that (27) is simply a choice we make, consistent with the flow equations, that turns out to be helpful.

Given this choice, we can now uncover the effective propagator relation. Using (27) and (19), we note that (26) simplifies, since $\Sigma_{0RS}^{\ f\,f} = -S_{0RS}^{\ f\,f}$. In the χ-sector, equation (26) becomes

$$\dot{S}_{0\,a\,b}^{\ \bar{\chi}\chi}(p) = -S_{0\,a\,c}^{\ \bar{\chi}\chi}(p)\dot{\Delta}_{c\,d}^{\bar{\chi}\chi}(p)S_{0\,d\,b}^{\ \bar{\chi}\chi}(p), \tag{28}$$

Integrating up, we set the integration constant to zero to ensure that the integrated kernel for the massive field χ is well behaved as $p \to 0$. This yields:

$$S_{0\,a\,c}^{\ \bar{\chi}\chi}(p)\Delta_{c\,b}^{\bar{\chi}\chi}(p) = \delta_{ab}. \tag{29}$$

In other words, the integrated χ kernel is the inverse of the two-point, tree level vertex, in the χ-sector. In recognition of this relationship, we call $\Delta^{\bar{\chi}\chi}(p)$ an effective propagator. Indeed, in this sector of the calculation the effective propagator is essentially a propagator in the usual sense. However, that this is the case is due to a succession of choices we made purely for convenience. Moreover, in the A-sector we cannot even define a propagator in the usual sense, since we have not fixed the gauge. Consequently, we use the terminology 'effective propagator' to highlight the similarity of these object to normal propagators, mindful that this relationship should not be taken for granted.

In the A-sector, matters are slightly more complex. Equation (26) becomes

$$\dot{S}_{0\mu\,\nu}^{\;\;AA}(p) = -S_{0\mu\,\alpha}^{\;\;AA}(p)\dot{\Delta}^{AA}(p)S_{0\alpha\,\nu}^{\;\;AA}(p). \tag{30}$$

Now, from the Ward identity (10), the two-point, tree level vertex must be transverse. Thus, by dimensions, it must take the form

$$S_{0\mu\,\nu}^{\;\;AA}(p) = \frac{\Box_{\mu\nu}(p)}{c_p}, \tag{31}$$

where $\Box_{\mu\nu}(p) \equiv p^2\delta_{\mu\nu} - p_\mu p_\nu$ is the usual transverse kinetic term and $c_p \equiv c(p^2/\Lambda^2)$ is a dimensionless, smooth cutoff function. Substituting (31) into (30), noting that $\Box_{\mu\alpha}(p)\Box_{\alpha\nu}(p) = p^2\Box_{\mu\nu}(p)$ and integrating up we obtain

$$c(p) = p^2\Delta^{AA}(p),$$

where we have set the integration constant to zero to ensure that the effective propagator is well behaved as $p \to \infty$ [1]. Thus, in the A-sector, the effective propagator relation takes the form

$$S_{0\mu\,\nu}^{\;\;AA}(p)\Delta^{AA}(p) = \delta_{\mu\nu} - \frac{p_\mu p_\nu}{p^2}; \tag{32}$$

in other words, the effective propagator is only the inverse of the two-point, tree level vertex in the transverse space.

We have purposely left the ψ sector until last, since there is a subtlety here. The point is that since ψ is a massless fermion (and we do not require the kinetic term to be regulated by a cutoff function), we can choose the seed action such that $S_0^{\;\bar{\psi}\psi}(p)$ is actually independent of Λ. In this case, we choose the integration constant in the ψ-sector version of (28) such that we have the relationship

$$S_{0\,a\,c}^{\;\;\bar{\psi}\psi}(p)\Delta_{c\,b}^{\bar{\psi}\psi}(p) = \delta_{ab}. \tag{33}$$

The three equations (29), (32) and (33) can be combined into

$$S_{0MR}^{\;\;XY}(p)\Delta_{RN}^{YZ}(p) = \delta_{MN} - p'_M p_N \tag{34}$$

where we use the following prescription for interpreting the various elements of this equation in different sectors:

1. in the A-sector, the indices are all Lorentz indices, $\Delta_{RN}^{YZ}(p)$ is just $\Delta^{YZ}(p)\delta_{\rho\nu}$ and $p'_M = p_\mu/p^2$ and $p_N = p_\nu$;
2. in the ψ and χ-sectors, all indices are spinor indices but p'_M and p_N are null.

We call the structure $p'_M p_N$ a 'gauge remainder'. This captures the notion that the pure gauge effective propagator leaves something behind, other than a Kronecker-δ, when contracted into a two-point, tree level vertex. Equation (34) is represented diagrammatically in figure 8, where a dummy effective propagator is denoted by a long, solid line.

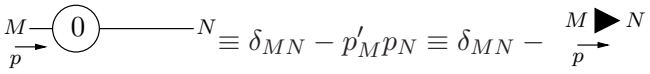

$$\equiv \delta_{MN} - p'_M p_N \equiv \delta_{MN} - \tag{35}$$

Figure 8: The effective propagator relation.

We conclude this section by giving explicit algebraic realisations (that correspond to the regularisation described in appendix A) for the two-point, tree level vertices and effective propagators which are summarised, together with the gauge remainders, in table 1.

	$S_{0MN}^{ff}(p)$	$\Delta^{ff}(p)$	p'_M	p_N
A	$\dfrac{\Box_{\mu\nu}(p)}{c_p}$	$\dfrac{c_p}{p^2}$	$\dfrac{p_\mu}{p^2}$	p_ν
ψ	$\not{p}$	$\dfrac{1}{\not{p}}$	—	—
χ	$\not{p}+\Lambda$	$\dfrac{1}{\not{p}+\Lambda}$	—	—

Table 1: Algebraic realisation of the two-point, tree level vertices, effective propagators and gauge remainders.

There are several things to note. First, the renormalisation condition (2) demands that

$$c_0 = 1. \tag{36}$$

Secondly, it is indeed the case that $\dot{\Delta}^{\bar{\psi}\psi}$ vanishes.

5 Computing β_1

5.1 The Starting Point

The key to extracting β-function coefficients from the weak coupling flow equations (24) is to use the renormalisation condition (2), which places a constraint on the vertex $S^{AA}_{\mu\,\nu}(p)$. From equations (17) and (36) and table 1, this constraint is saturated at tree level:

$$S^{AA}_{\mu\,\nu}(p) = \frac{1}{e^2}\Box_{\mu\nu}(p) + \mathcal{O}(p^4) = \frac{1}{e^2}\frac{\Box_{\mu\nu}(p)}{c_0} + \mathcal{O}(p^4) = \frac{1}{e^2}S_{0\mu\,\nu}^{\;\;AA}(p).$$

Hence, all higher loop two-point vertices, $S_{n\geq 1\mu\,\nu}^{\;\;AA}(p)$ vanish at $\mathcal{O}(p^2)$.

To utilise this information, we specialise equation (24) to compute the flow of $S_{1\mu\,\nu}^{\;\;AA}(p)$:

$$\dot{S}_{1\mu\,\nu}^{\;\;AA}(p) = -2\beta_1 S_{0\mu\,\nu}^{\;\;AA}(p) + \sum_{r=0}^{1} a_0[\bar{S}_{1-r}, \bar{S}_r]^{AA}_{\mu\,\nu}(p) - a_1[\Sigma_0]^{AA}_{\mu\,\nu}(p). \tag{37}$$

Now we focus on the $\mathcal{O}(p^2)$ part of this equation. The term on the l.h.s., being a two-point gauge vertex of loop order greater than zero, vanishes at $\mathcal{O}(p^2)$. On the r.h.s., the a_0 term can be discarded. Recall that this term comprises two vertices joined together by an ERG kernel (cf. figure 5). We must decorate each of these vertices with one of the external fields, A_μ or A_ν, else one of vertices is one-point vertex and these do not exist. However, if we decorate both vertices with a single external field then, by gauge invariance, they are both transverse in p and so the diagram is at least $\mathcal{O}(p^4)$.

Equation (37) collapses to an algebraic expression for β_1:

$$2\beta_1\Box_{\mu\nu}(p) + \mathcal{O}(p^4) = -a_1[\Sigma_0]^{AA}_{\mu\,\nu}(p), \tag{38}$$

which is shown diagrammatically in figure 9, employing the notation of figure 4. It is taken as understood in all that follows that the external indices are μ and ν and we are working at $\mathcal{O}(p^2)$.

Diagrams are labelled in boldface. If a diagram is cancelled, then its reference number is enclosed in curly braces, together with the reference number of the diagram against which it cancels. If the reference number of a diagram is followed by an arrow, it can mean one of two things:

1. $\rightarrow 0$ denotes that the corresponding diagram can be set to zero, for some reason;

2. $\rightarrow$ followed by a number (other than zero) indicates the number of the figure in which the corresponding diagram is processed.

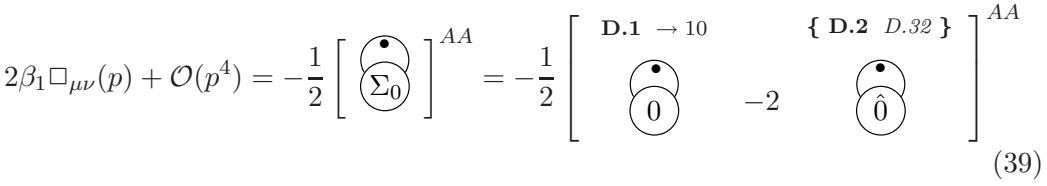

Figure 9: A diagrammatic representation of the equation for β_1. On the r.h.s., we implicitly take the indices to be μ and ν and work at $\mathcal{O}(p^2)$.

5.2 Diagrammatic Manipulations

As it stands, we cannot directly extract a value for β_1 from equation (39). The r.h.s. is phrased in terms of non-universal objects. Whilst one approach would be to choose a particular scheme in which to compute these objects [3, 14] we anticipate from [1, 3, 6] that this is unnecessary: owing to the universality of β_1, all non-universalities must somehow cancel out. To proceed, we utilise the flow equations.

Our aim is to try and reduce the expression for β_1 to a set of Λ-derivative terms—terms where the entire diagram is hit by $-\Lambda\partial_\Lambda$—since, as we will see in section 5.3, such terms either vanish directly or give universal contributions (in the limit that $D \to 4$). Focusing on diagram D.1, we note that if both decorative fields decorate the vertex, then the internal line is just a differentiated effective propagator—in this case we can generate a Λ-derivative term by moving the $-\Lambda\partial_\Lambda$ from the effective propagator to the vertex.

Hence, our first task is to separate off the manipulable component of diagram D.1. To this end, we define an object called the *reduced* kernel:

$$\left(\dot{\Delta}\right)_R \equiv \mathring{\dot{\Delta}} = \dot{\Delta} - \dot{\Delta}^{XY}_{ST}(k), \tag{40}$$

where we have suppressed all arguments of the generic kernel, $\dot{\Delta}$, and its reduction, $\mathring{\dot{\Delta}}$. In figure 10 we re-express diagram D.1.

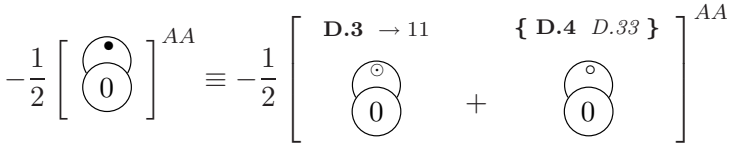

Figure 10: Isolating the manipulable component of diagrams D.1.

The symbol $\odot$ tells us that the corresponding kernel is not decorated, whereas the symbol $\circ$ means the converse. We now convert diagram D.3 into a Λ-derivative term, as shown in figure 11.

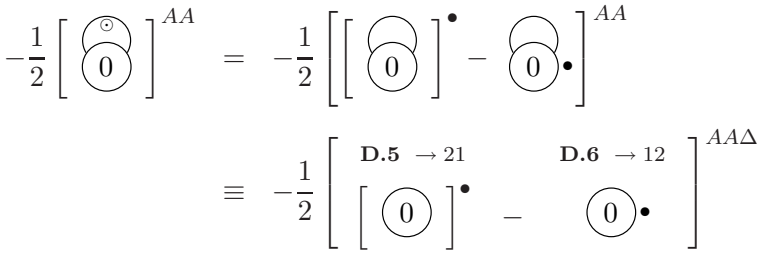

Figure 11: The manipulation of diagram D.3.

Notice that, on the second line, we have refined the notation further, by promoting the effective propagator in both diagrams to an implicit decoration. This must be done with care. In diagram D.5, the vertex is enclosed in square brackets which tells us that $-\Lambda\partial_\Lambda$ is take to act *after explicit decoration*. However, in diagram D.6, it is just the vertex which is struck by $-\Lambda\partial_\Lambda$. Diagram D.5 is one of the Λ-derivative terms we have been looking for.

The next step is to process diagram D.6, using the tree level flow equations. This is shown in figure 12.

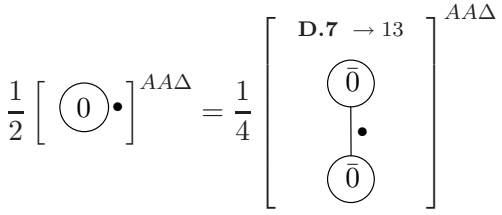

Figure 12: The manipulation of diagram D.6.

A word is in order about the rules for decorating diagram D.7 [3]. Let us start with the external fields. If we attach each of these to a different structure, we pick up a factor of two; if we attach them to the same structure, the combinatoric factor

is just unity. Similarly, if the ends of the effective propagator attach to different structures then we pick up a factor of two; if they do not then the combinatoric factor is unity.

To proceed further, we now isolate all two-point, tree level vertices (there was no need to do this when manipulating diagram D.1, since the vertex of this diagram is compelled to be four-point). The reason we do this is that we do not wish to process such vertices via the flow equations; rather, if we attach them to effective propagators, then we can use the effective propagator relation. Alternatively, if we decorate them with external fields, we will be able to use the fact that they are manifestly $\mathcal{O}(p^2)$.

To facilitate this separation, we define reduced, tree level vertices, thus:

$$v_0^R = v_0 - v_{0RS}^{ff}(k),$$

where we have suppressed all arguments of the generic vertex v_0 and its reduction, v_0^R. We now re-express diagram D.7, as in figure 13, recalling the notation of figure 6. Notice that, for those diagrams possessing two-point, tree-level, vertices, we have expanded out the bar-notation according to (23):

$$a_0[\bar{S}_0, \bar{S}_0^2] = a_0[S_0, S_0^2] - a_0[S_0, \hat{S}_0^2] - a_0[\hat{S}_0, S_0^2] = -a_0[\hat{S}_0, S_0^2],$$

where the cancellation of terms occurs due to the equality of the Wilsonian effective action and seed action two-point, tree level vertices.

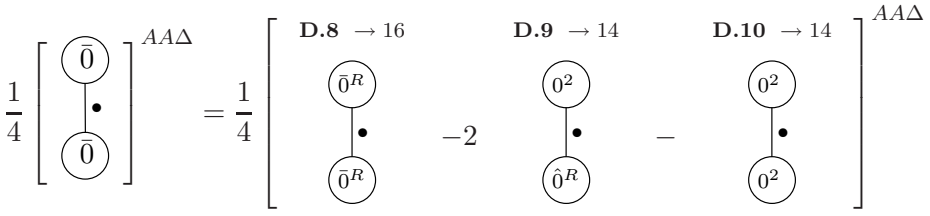

Figure 13: Isolating the two-point, tree level vertices of diagram D.7.

Our strategy now is to decorate the two-point, tree level vertices of diagrams D.9 and D.10. For each such vertex we can attach one of two things: either an end of the effective propagator or an external field. In the former case, we must now join up the loose end of the effective propagator. This can never attach to the kernel, as we now argue. The key point is that only χ or ψ-sector kernels have decorations and that these decorations must be As. Thus, trying to join one end of the effective

propagator to the kernel and the other end to a two-point, tree level vertex would mean that the vertex would have to be decorated by an A and one of the spinor fields; such vertices do not exist. Consequently, having attached one end of the effective propagator to a two-point, tree level vertex, the other end must attach to the other vertex.

We can attach an external field to the two-point, tree level vertex of diagram D.9 but we cannot do likewise in diagram D.10. Performing this decoration forces the kernel to be in the A-sector; hence the kernel cannot be decorated. But, in diagram D.10, this would mean that it is not possible to perform the explicit decorations, as there are too many fields and not enough legal locations.

The result of the partial decoration of diagrams D.9 and D.10 is shown in figure 14.

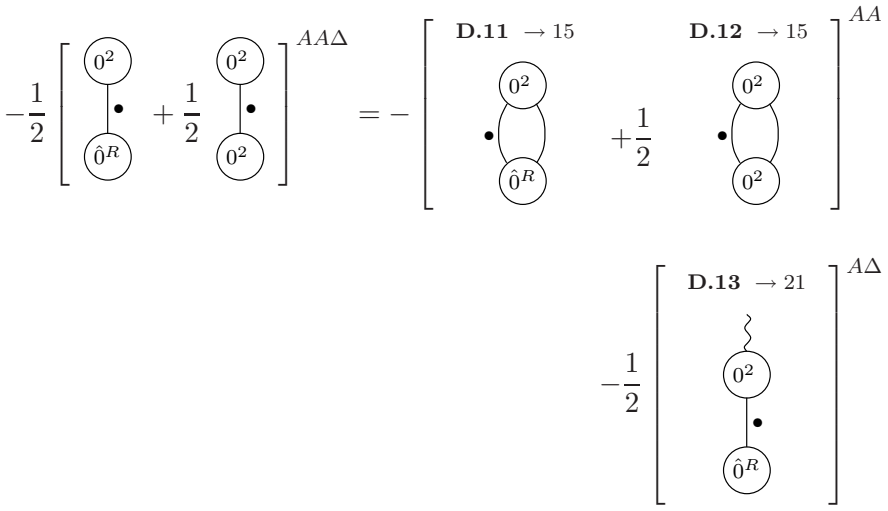

Figure 14: Result of decorating the two-point, tree level vertices of diagrams D.9 and D.10.

We now reach the crux of the entire diagrammatic approach: diagrams D.11 and D.12 can be processed using the effective propagator relation (35) upon which, the calculation starts to simplify. This is shown in figure 15.

Diagram D.15 can be discarded: for the gauge remainder to have support, it must be in the A-sector (see table 1). However, this means that the vertex is pure A and so is killed by the gauge remainder, courtesy of the Ward identity (10). Diagram D.17

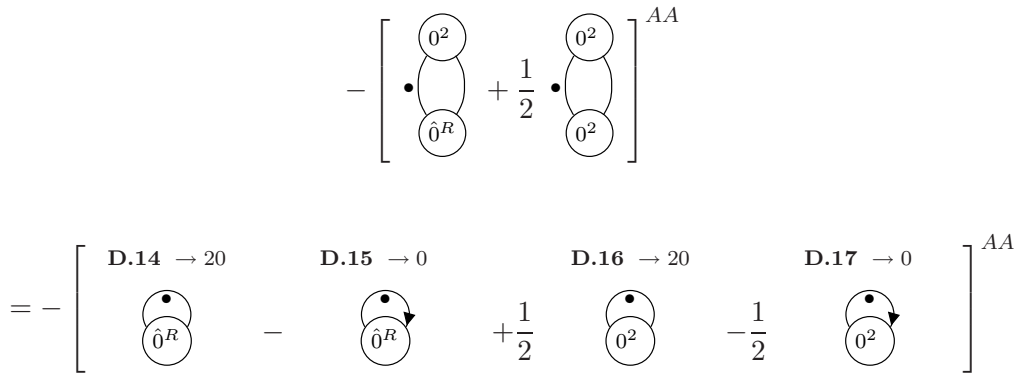

Figure 15: Applying the effective propagator relation to diagram D.11.

can be discarded: the kernel is decorated, meaning that it must be in either the ψ or χ-sectors and so the gauge remainder has no support.

Our strategy now is simple: we iterate the diagrammatic procedure. We begin by taking diagram D.8 and isolating the manipulable component i.e. the component which possesses only Wilsonian effective action vertices and an undecorated kernel. This is shown in figure 16.

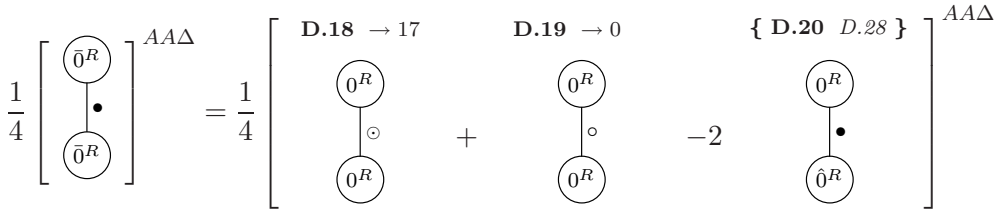

Figure 16: Isolating the manipulable component of diagram D.8.

Diagram D.19 can be discarded. Since one-point vertices do not exist, and the vertices cannot be two-point (by the definition of a reduced vertex), both vertices must be at least three-point. But, upon explicit decoration, this does not leave behind any fields to decorate the (reduced) kernel.

In figure 17, we convert diagram D.18 into a Λ-derivative term.

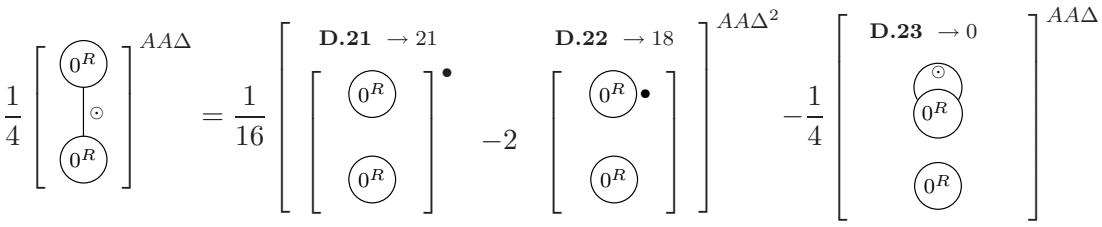

Figure 17: Converting diagram D.18 into a Λ-derivative term.

The overall factors in front of the daughter diagrams require explanation [3]. In going from the parent diagram, D.18, to the daughters, we have moved the $-\Lambda\partial_\Lambda$ off the effective propagator. This effective propagator has subsequently been promoted to an implicit decoration. Immediately, we pick up a factor of 1/2 in recognition of the fact that the effective propagator can be reattached, so as to join the two vertices back together, either way round. We now have two, identical effective propagators amongst our implicit decorations. To recreate the parent diagram, we can choose either of these effective propagators to be hit by $-\Lambda\partial_\Lambda$ and so we must compensate with a further factor of 1/2. This explains why diagram D.21 comes with a relative factor of 1/4, compared to the parent. As for diagram D.22 the $-\Lambda\partial_\Lambda$ can strike either of the vertices, with the same effect; we combine these terms, to yield a factor of two.

Let us now consider diagram D.23, the final correction generated when we convert the parent diagram into the Λ-derivative term, D.21. Diagram D.23 can be formed in four ways: the $-\Lambda\partial_\Lambda$ can strike either of the effective propagators, and we can form a loop with the differentiated effective propagator on either of the vertices. Diagram D.23 can be discarded. To make a complete diagram, we must join the two vertices together, using the effective propagator, which must be in the A-sector. Since the bottom vertex is reduced, and one-point vertices do not exist, it must also be decorated by both of the external fields. Hence, the bottom vertex is a pure gauge, three-point vertex, which vanishes as a consequence of charge conjugation invariance (equivalently, Furry's theorem [15]).

Now we process diagram D.22. To do this, we must understand how to compute the flow of a reduced vertex. This is easy. Remember that a reduced vertex does not have a two-point, tree level term. From section 4.2, we know that the flow of a two-point, tree level vertex produces a pair of two-point, tree level vertices joined together by a differentiated effective propagator. This diagram must be excluded from the flow of a reduced vertex, meaning that either at least one of the vertices must be reduced or the kernel must be decorated. In figure 18 we show the result of

processing diagram D.22.

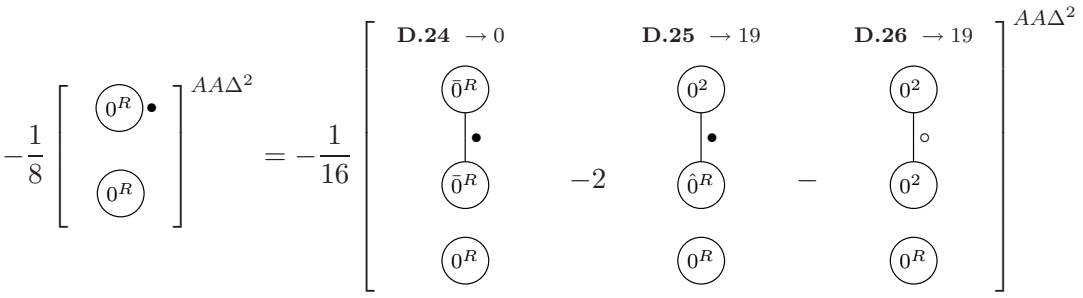

Figure 18: The result of processing diagram D.22.

Diagram D.24 can be discarded. All three vertices of this diagram are reduced and there are not enough implicit decorations to avoid one of them being either one-point, which does not exist, or two-point, which is forbidden by the reduction.

Now we decorate the two-point, tree level vertex of diagram D.25. When doing so with an effective propagator, we pick up a factor of four: one factor of two to recognise that we could have attached either effective propagator and one factor of two because the ends of the effective propagator attach to different structures. This time, we utilise the effective propagator relation immediately and again recognise that all gauge remainders can be discarded.

Finally, we decorate the two-point, tree level vertices of diagram D.26. Since the kernel must be decorated—and so must be in the ψ or χ-sectors—we cannot decorate either of the two-point, tree level vertices with an external field. Consequently, we must either attach a separate effective propagator to each or we must join the two vertices together with a single effective propagator. Again, we utilise the effective propagator relation immediately and recognise that all gauge remainders can be discarded. We thus obtain the diagrams of figure 19.

Cancellation 1 *Diagram D.28 exactly cancels diagram D.20.*

Diagrams D.29 and D.30 can be discarded for exactly the same reason as diagram D.23. The final diagrammatic step is to combine diagrams D.14, D.16 and D.31, as shown in figure 20. We utilise the fact that the two-point, tree level, Wilsonian effective action vertices are equal to the corresponding seed action vertices and also that those diagrams in which the vertex is two-point necessarily have a reduced (i.e. decorated) kernel.

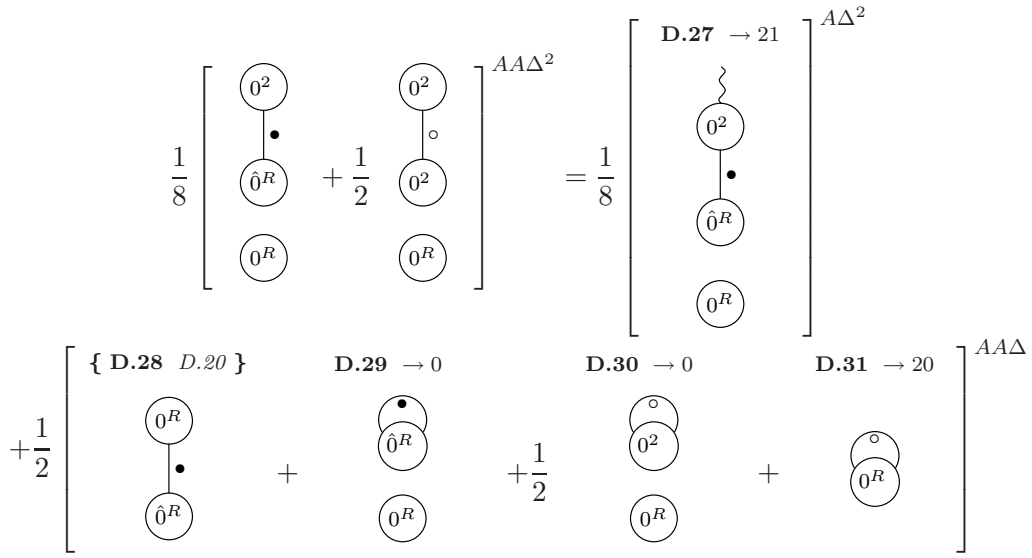

Figure 19: Result of decorating the two-point, tree level vertices of diagrams D.25 and D.26.

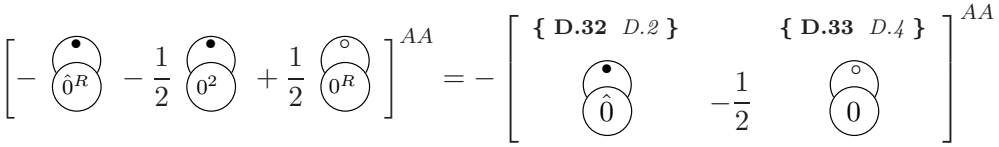

Figure 20: Result of combining diagrams D.14, D.16 and D.31.

Cancellation 2 *Diagram D.32 exactly cancels diagram D.2.*

Cancellation 3 *Diagram D.33 exactly cancels diagram D.4.*

The only surviving terms are diagrams D.5, D.13, D.21 and D.27. We now explicitly decorate these diagrams and, throwing away any terms which vanish due to charge conjugation invariance, arrive at figure 21.

A number of comments are in order. All fields in diagram D.34 attach to the same vertex and so we do not pick up any factors upon decoration. In diagram D.35, each of the effective propagators can be attached either way round, giving a factor

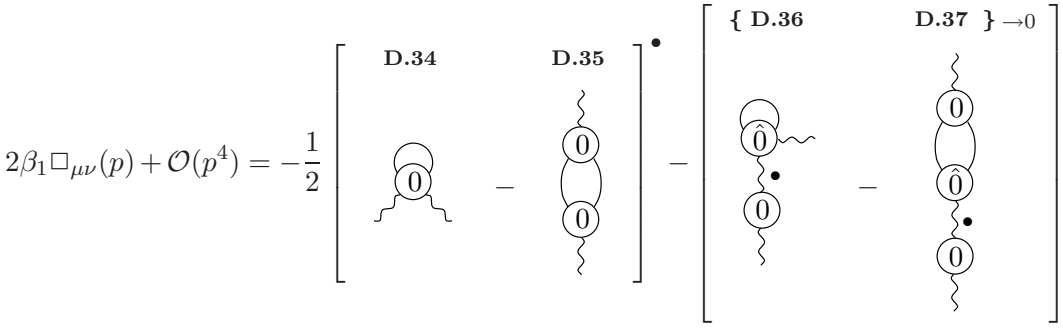

Figure 21: The surviving contributions to β_1.

of four. The external fields attach to different vertices, yielding a further factor of two.

In diagrams D.36 and D.37 we recognise that the internal field leaving the two-point, tree level vertex must be in the A-sector. Let us now analyse these diagrams in more detail. The two-point, tree level vertex is, from table 1, at least $\mathcal{O}(p^2)$ and so, since we are working at $\mathcal{O}(p^2)$, we are compelled to take $\mathcal{O}(p^0)$ from the rest of each of the diagrams. This is no problem for the differentiated effective propagator, which will contribute $\sim c_0'$. However, we can straightforwardly demonstrate [3] using the Ward identities (10) and (11) and the effective propagator relation, that the sum of the diagrams to which the top end of the effective propagator attaches are transverse in p—and hence at least $\mathcal{O}(p^2)$.[2] Thus, the sum of diagrams D.36 and D.37 is at least $\mathcal{O}(p^4)$ and so does not contribute to β_1. That this is the case is just as well: c_0' is non-universal and its inverse cannot be generated by loop integration.

5.3 The Λ-derivatives

5.3.1 Strategy

From figure 21, our equation for β_1 can be written in the form:

$$2\beta_1\Box_{\mu\nu}(p)=-\frac{1}{2}\left[\mathcal{D}_1\right]^\bullet.$$

[2]This can be seen by contracting the four point vertex of diagram D.36 with the momentum of one of the external fields and likewise for the top-most three-point vertex of diagram D.37. In the latter case, this procedure generates two-point vertices to which we can apply the effective propagator relation.

We now want to make the integral over loop momentum (which we will take to be k) to be explicit and so write

$$2\beta_1 \Box_{\mu\nu}(p) = -\frac{1}{2}\int_k [\mathcal{D}_1(k)]^\bullet \,. \tag{41}$$

The next step that we wish to perform is to interchange the order of the Λ-derivative and the momentum integral. This step is trivial only if the integral is convergent, even after this change. We temporarily ignore this subtlety and so now have

$$2\beta_1 \Box_{\mu\nu}(p) = -\frac{1}{2}\left[\int_k \mathcal{D}_1(k)\right]^\bullet .$$

Since the l.h.s. of this equation comprises a number times $\mathcal{O}(p^2)$, it follows that the coefficient multiplying the $\mathcal{O}(p^2)$ part of the r.h.s. must be dimensionless. Consequently, we can schematically write

$$\beta_1 = -\Lambda\partial_\Lambda \,(\text{Dimensionless Quantity})\,.$$

For the r.h.s. to survive differentiation with respect to Λ, it must either depend on some dimensionless running coupling—other than e—or there must be some scale, other than Λ, available for the construction of dimensionless quantities. We show in appendix B that no such running couplings exist.

One scale which is available is p and so we can envisage contributions to β_1 of the form (in $D = 4$)

$$-\Lambda\partial_\Lambda \ln p^2/\Lambda^2.$$

Indeed, one can arrange the calculation precisely so as to obtain just such a contribution. However, there is an easier way to proceed. We note that the l.h.s. of equation (41) is Taylor expandable in p and so it must be the case that the r.h.s. is Taylor expandable too. Let us suppose that we were to Taylor expand $\mathcal{D}_1$ in equation (41) i.e. *before* we have interchanged the order of loop integration and differentiation with respect to Λ.

If we now try and change the order of loop integration and differentiation with respect to Λ we must be very careful, since this procedure has the capacity to introduce divergences in both the IR and UV—we comment further on this shortly. Thus, to legally move $-\Lambda\partial_\Lambda$ outside of the loop integral in the case where we have Taylor expanded in p, we must introduce some regulator. This then provides the scale necessary to form dimensionless quantities. After allowing $-\Lambda\partial_\Lambda$ to act, this unphysical scale will disappear. As we are already working in dimension D, it is natural to use dimensional regularisation as our regulator.

We are now able to see the effects of keeping diagrams generated by the ψ-sector terms in the flow equation (recall that, since $\dot{\Delta}^{\bar{\psi}\psi} = 0$, these could have been discarded). If we keep them then, after first Taylor expanding in p and next interchanging the order of loop integration and differentiation, $\int_k \mathcal{D}_1(k)$ is still convergent in the UV but diverges in the IR. Had we discarded the ψ-sector diagrams, then $\int_k \mathcal{D}_1(k)$ would diverge in the UV but converge in the IR. Either way, the contribution to β_1 in the $D \to 4$ is the same, but we have a choice about how to compute it.

For the purposes of QED, it makes no difference whether we extract β_1 from the IR or the UV of $\int_k \mathcal{D}_1(k)$ (though, in the former case, it makes it clear how universal contributions are controlled by the renormalisation condition). However, in Yang-Mills theory, there are only a subset of diagrams for which we have this choice; the rest yield contributions from the IR only [1, 3]. Consequently, in Yang-Mills, it makes sense to evaluate all contributions to β-function coefficients in the IR. As the purpose of this paper is to introduce and illustrate the Yang-Mills methodology, we will choose to compute in the IR here, too.

With this in mind, our strategy for extracting β_1 is as follows. First, we Taylor expand all diagrams to $\mathcal{O}(p^2)$. Then we focus on the IR divergent part of the integral, throwing all other contributions away (since these will vanish in the limit that $D \to 4$).

5.3.2 Numerical Evaluation

Let us start by looking at diagram D.34. This has a single effective propagator which, scanning through table 1, will blow up when $p \to 0$ in the ψ or A-sectors. However, this is not enough to generate an IR divergence, and so the diagram vanishes in the $D \to 4$ limit.

Finally, let us look at diagram D.35. In the pure gauge sector, this diagram does not even exist, since three-point pure gauge vertices vanish. The diagram does exist in the ψ and χ-sectors. The severe IR behaviour occurs in the ψ-sector and so we expect to be able to throw the χ-sector diagram away. We can do this, but must be careful: the χ-sector diagram regulates the ψ-sector diagram in the UV. We can throw away the χ-sector diagram if we incorporate the effects of the UV regularisation. This is done by replacing the upper limit of the radial integral by Λ for the ψ-sector diagram, which is valid up to (non-universal) corrections which vanish as $D \to 4$ [3]. We now rescale $k \to k/\Lambda$, so that the upper limit of the radial integral becomes unity, and the diagram acquires an overall factor of $\Lambda^{-2\epsilon}$.

Recalling the Feynman rules of section 3.2 for diagrams possessing internal ψs, diagram D.35 reduces to

$$-\left[\Lambda^{-2\epsilon}\right]^{\bullet} \int_0^1 dk k^{D-1} \int d\not{\Omega}_D \text{ tr } \left[S_0{}^{\bar{\psi}\psi A}_{\mu}(-p-k,k,p) \frac{1}{\not{k}} S_0{}^{\bar{\psi}\psi A}_{\nu}(-k,p+k,-p) \frac{1}{\not{p}+\not{k}} \right]_{p^2},$$

where the notation $f|_{p^2}$ signifies that the $O(p^2)$ in the series expansion of f must be taken and $\not{\Omega}_D$ is the area of the unit sphere in D dimensions, divided by $(2\pi)^D$. The leading IR behaviour comes from taking the $\mathcal{O}(p^2)$ part of $1/(\not{p}+\not{k})$, and so we must set $p=0$ in the vertices. Now, setting p to zero in this manner allows us to relate the three-point vertices to two-point vertices via the Ward identity (11).

Indeed, specialising (11) to the momenta $\{-k-\eta, k, \eta\}$ with η infinitesimal yields

$$\eta^\mu S_0{}^{\bar\psi\psi A}_{\quad\mu}(-k-\eta,k,\eta) = S_0{}^{\bar\psi\psi}(-k-\eta) - S_0{}^{\bar\psi\psi}(-k), \tag{42}$$

from which one immediately obtains $S_0{}^{\bar\psi\psi A}_{\quad\mu}(-k,k,0) = \partial^k_\mu S_0{}^{\bar\psi\psi}(-k)$ by expanding to first order in η.

We therefore have that

$$2\beta_1 \Box_{\mu\nu}(p) = \left[\Lambda^{-2\epsilon}\right]^\bullet \int_0^1 dk k^{D-1} \int d\not{\Omega}_D \ \mathrm{tr}\left[\gamma_\mu \frac{\not{k}}{k^2}\gamma_\nu\left[2\not{p}\frac{k.p}{k^4} + \not{k}\left(\frac{p^2}{k^2} - 4\frac{(p.k)^2}{k^6}\right)\right]\right].$$

Taking the trace of the γ matrices and averaging over angles yields

$$2\beta_1 \Box_{\mu\nu}(p) = -4\ \not{\Omega}_D \frac{D-2}{D+2}\left[\Lambda^{-2\epsilon}\right]^\bullet \int_0^1 dk k^{-1-2\epsilon}\left[p^2\delta_{\mu\nu} - \frac{4}{D}p_\mu p_\nu\right],$$

from which we obtain, in the $D\to 4$ limit,

$$\beta_1 = \frac{1}{12\pi^2}.$$

A Regularisation

In this appendix, we justify the statement that QED is regularised by the introduction of the cutoff function c in the photon effective propagator and by the introduction of a massive bosonic spinor χ; the effective propagators are listed in table 1.

It is easy to appreciate intuitively that the regularised theory can be finite in $D=4$ dimensions, to all orders in perturbation theory: in a given diagram generated by the flow, every loop containing at least one photon effective propagator is regulated by the presence of the cutoff function (providing c decays strongly enough, as determined below) whereas the ultraviolet divergences in purely fermionic loops are cancelled by those coming from purely commuting spinor loops.

In order to prove that the regularisation is sufficient for the computations in this paper, we would need to further constrain the, so far largely undetermined, seed action $\hat{S}$. Rather than doing this, we follow the spirit of refs. [3, 6], leaving $\hat{S}$

largely undetermined but insisting that the underlying regularisation is sufficient to regularise the theory defined by the simplest bare action:

$$S_{\text{bare}} = \frac{1}{4e^2} F_{\mu\nu} \cdot c^{-1} \cdot F_{\mu\nu} + \frac{1}{e^2} \int d^D x \; [\bar{\psi}(i\partial\!\!\!/ + A\!\!\!/)\psi + \bar{\chi}(i\partial\!\!\!/ + \Lambda + A\!\!\!/)\chi] \,. \tag{43}$$

We will see that this is the case providing $c(x)$ decays faster than $1/x^2$. Although we do not prove it, it is undoubtedly true that the simplest $\hat{S}$ then also leads to a fully regularised theory. (A larger class of $\hat{S}$ will also result in regularised diagrams and by requiring c to decay faster even more general seed actions may be considered.)

Using (43), the worst case divergence from a ψ loop is the one-loop photon self-energy, which is quadratically divergent by power counting. However as is well known, this must be transverse [16], see also equation (10), and thus is only logarithmically divergent. This divergence is exactly cancelled by the opposite sign χ loop. The only other possible cause for concern would be the one-loop four-photon vertex (vertices with just an odd number of photons vanishing by Furry's theorem [15]) but again, as is well known [16], gauge invariance forces this diagram to be finite.

It remains only to show that c can be chosen to make all the other diagrams ultraviolet finite. We follow standard power counting techniques, adapting ref. [4]. Although we should gauge fix for this, the ghosts play no rôle, decoupling in both the Lagrangian and the Ward identities.

The superficial degree of divergence of any one-particle-irreducible diagram in D space-time dimensions, is given by

$$\mathcal{D}_\Gamma = DL - (2n+2)\, I_A - I_\psi - I_\chi, \tag{44}$$

where L is the number of loops and I_f stands for the number of internal lines of f-type. Note that the vertices from (43) do not enter (44) as they do not carry any momentum dependence.

The variables which $\mathcal{D}_\Gamma$ depends upon can be easily related to the number of external lines and vertices of each type—respectively E_f, V_f—as

$$\begin{aligned} L &= 1 + I_A + I_\psi + I_\chi - V_{\psi^2 A} - V_{\chi^2 A}, & (45)\\ E_A &= -2I_A + V_{\psi^2 A} + V_{\chi^2 A}, & (46)\\ E_{\bar{\psi}} &= -I_\psi + V_{\psi^2 A}, & (47)\\ E_{\bar{\chi}} &= -I_\chi + V_{\chi^2 A}. & (48) \end{aligned}$$

In equations (47) and (48), by $E_{\bar{\psi},\bar{\chi}} (= E_{\psi,\chi})$ we mean the number of external conjugate spinor lines.

Using the above formulae, we rewrite $\mathcal{D}_\Gamma$ so that it is independent of internal lines:

$$\mathcal{D}_\Gamma = (D-2n-4)\,(L-2) - E_A - (2n+3)\, E_{\bar{\psi}} - (2n+3)\, E_{\bar{\chi}} + 2(D-n-2). \tag{49}$$

In order for every possible $L \geq 2$ loop 1PI diagram to have a negative $\mathcal{D}_\Gamma$, one can impose all coefficients in (49) to be negative and, thus, get sufficient conditions. This results in a lower bound for n,

$$n > D - 2. \tag{50}$$

Such a condition is also necessary if one relies on power counting arguments only, as $2(D - n - 2)$ represents the actual degree of divergence of the two-loop vacuum diagram made from two three-point vertices (the so-called no-go diagram).

For the one-loop diagrams we set $L = 1$ and, rearranging some of its terms, it is easy to show that diagrams containing at least one external conjugate spinor and those with more than D external photons are finite provided n satisfies (50). On the contrary, one-loop diagrams with up to D external photons and no external $\bar{\psi}$ or $\bar{\chi}$ cannot be regulated this way, whatever the choice of n, since $\mathcal{D}_\Gamma$ is then $D - E_A$. In four dimensions, these are just the one-loop two-point and four-point photon vertices that we have already explained are finite.

We have thus shown that providing $n > 2$, the theory defined by (43) is finite to all orders in perturbation theory in $D = 4$ dimensions.

B Dimensionless Running Couplings

Consider the flow of any vertex with mass dimension ≥ 0. Taylor expand in momenta and focus on the term which is the same order in momenta as the mass dimension of the vertex. The coefficient of this term must be dimensionless. We now demonstrate that the flow of all such coefficients vanishes. The only candidates are as follows, where we indicate the power of momentum that we must take from the vertex:

$$S^{\bar{\psi}\psi}(k)\Big|_{\mathrm{mom}^1}, \qquad S^{\bar{\psi}\psi A}{}_{\mu}(k, p-k, p)\Big|_{\mathrm{mom}^0}, \qquad S^{AA}_{\mu\,\nu}(k)\Big|_{\mathrm{mom}^2}, \qquad \psi(\bar{\psi}) \to \chi(\bar{\chi}).$$

(Of the other potential candidates, S^{AAA} does not exist by charge conjugation invariance and S^{AAAA} does not have an $\mathcal{O}\left(\mathrm{mom}^0\right)$ component since, by gauge invariance, it is transverse on all legs.)

The point is that all of these vertices, expanded to the order in momenta indicated, are controlled by the renormalisation condition (2) and so can immediately be shown to be independent of Λ. Therefore, there are no dimensionless running coupling constants, besides e.

Acknowledgements TRM and OJR acknowledge financial support from PPARC Rolling Grant PPA/G/O/2002/0468. TRM is grateful for support from a CERN paid scientific associateship during this research. SA would like to thank Massimo Testa and Kensuke Yoshida for their enthusiasm and interest.

References

[1] S. Arnone, A. Gatti and T. R. Morris, *Phys. Rev.* **D 67** (2003) 085003, [hep-th/0209162].

[2] O. J. Rosten, T. R. Morris and S. Arnone, The Gauge Invariant ERG, Proceedings of Quarks 2004, Pushkinskie Gory, Russia, 24-30 May 2004, http://quarks.inr.ac.ru, [hep-th/0409042].

[3] O. J. Rosten, 'The Manifestly Gauge Invariant Exact Renormalisation Group', Ph.D. Thesis, [hep-th/0506162]; S. Arnone, T. R. Morris and O. J. Rosten, [hep-th/0507154].

[4] S. Arnone, Y. A. Kubyshin and T. R. Morris, J. F. Tighe, *Int. J. Mod. Phys.* **A 17** (2002) 2283, [hep-th/0106258].

[5] J.I. Latorre and T. R. Morris, *JHEP* 0011 (2000) 004, [hep-th/0008123].

[6] S. Arnone, A. Gatti, T. R. Morris and O. J. Rosten, *Phys. Rev.* **D 69** (2004) 065009, [hep-th/0309242].

[7] T. R. Morris, *Nucl. Phys.* **B 573** (2000) 97, [hep-th/9910058].

[8] T. R. Morris, *Nucl. Phys.* **B 495** (1997) 477, [hep-th/9612117].

[9] K. Wilson and J. Kogut, *Phys. Rep.* **12 C** (1974) 75.

[10] D. V. Shirkov, *Theor. Math. Phys.* **60** (1985) 778.

[11] T. R. Morris, *Prog. Theor. Phys. Suppl.* 131 (1998) 395, [hep-th/9802039].

[12] S. Arnone, A. Gatti and T. R. Morris *JHEP* 0205 (2002) 059, [hep-th/0201237].

[13] O. J. Rosten, in preparation.

[14] T. R. Morris, *JHEP* 0012 (2000) 012, [hep-th/0006064].

[15] H. Furry, *Phys. Rev.* **51** (1937) 125.

[16] C. Itzykson and J. B. Zuber, 'Quantum Field Theory' (1985) McGraw-Hill, Singapore.